

MOL #102723

Thrombin-mediated direct activation of proteinase-activated receptor-2 (PAR2): another target for thrombin signaling

Koichiro Mihara, Rithwik Ramachandran, Mahmoud Saifeddine, Kristina K. Hansen, Bernard Renaux, Danny Polley, Stacy Gibson, Christina Vanderboor and Morley D. Hollenberg

Inflammation Research Network-Snyder Institute for Chronic Disease, Department of Physiology & Pharmacology (KM, RR, MS, KKH, BR, DP, SG, MDH), and Department of Medicine (MDH), University of Calgary Cumming School of Medicine, Calgary AB Canada T2N 4N1, Department of Physiology and Pharmacology (CV, RR), Western University, London ON Canada N6A 5C1

MOL #102723

Running Title: Direct thrombin activation of PAR2

Corresponding Author:

Morley D. Hollenberg

Department of Physiology & Pharmacology

University of Calgary Cumming School of Medicine

3330 Hospital Drive NW

Calgary AB Canada T2N 4N1

Phone: 403-220-6931; cell 403-669-6954

FAX: 403-270-0979

Email: mhollenb@ucalgary.ca

Text Details:

Text Pages: 20

Tables: 0

Figures: 6

References: 27

Abstract: 150 words

Introduction: 824 words

Results & Discussion: 2318 words total. 1782 words results; 536 words discussion section

ABBREVIATIONS USED

Amino acids are abbreviated by their one-letter codes, e.g. L = leucine, S = serine; **CRISPR**: clustered regularly interspaced short palindromic repeats; **ERK 1/2**: Extracellular-regulated protein kinase 1/2 (p42/44 MAPKinase); **2fLI**: 2-furoyl-LIGRLO-NH₂, a PAR2-selective receptor-activating peptide; **HEK**: Human embryonic kidney-derived cells; **HBSS**: Hank's Buffered salt solution; **HTB-9**: Bladder cancer-derived cell line; **KNRK**: Kirsten-virus-transformed normal rat kidney cells; **nLuc or Nluc**: NanoLuc luciferase ; **rLUC**: Renilla luciferase ; **MAPK or MAPKinase**: Mitogen-activated protein kinase (ERK 1/2); **P1N**: PAR1-null HEK cells; **P1Null-HEK or P1N-HEK**: HEK cells in which PAR1 has been eliminated by the CRISPR approach; **P1N-HEKPAR2-Y**: PAR1-null HEK cells transfected with wild-type PAR2 having a C-terminal YFP tag; **P1N-HEKPAR2-Y-R/A**: PAR1-null HEK cells transfected with an arginine to alanine mutation at the R36 cleavage-activation site of PAR2 that also has a C-terminal YFP; **P1N-HTB-9**: PAR1-null HTB-9 cells; **PAR**: Proteinase-activated receptor (PAR1, PAR2); **RFP or mRFP**: Red fluorescent protein monomer; **RFP-P2Y**: HEK cells expressing dually tagged N-terminal mRFP/C-terminal YFP PAR2; **RFP-P2Y-R/A**: HEK cells expressing dually tagged N-terminal mRFP/C-terminal YFP PAR2 with an R36A mutation at the tryptic tethered ligand cleavage site; **TF**: TFLLR-NH₂, a PAR1-selective receptor-activating peptide; **TL**: A 'tethered ligand' PAR-activating sequence unmasked in the course of proteolytic activation of a PAR; **YFP or eYFP**: Enhanced yellow fluorescent protein

MOL #102723

ABSTRACT

Thrombin is known to signal to cells by cleaving/activating a G-protein-coupled family of proteinase-activated receptors (PARs). The signaling mechanism involves the proteolytic unmasking of an N-terminal receptor sequence that acts as a ‘tethered’ receptor-activating ligand (TL). To date, the recognized targets of thrombin cleavage-activation for signaling are PARs 1 and 4, in which thrombin cleaves at a conserved target arginine to reveal a tethered ligand. PAR2, which like PAR1 is also cleaved at an N-terminal arginine to unmask its tethered-ligand, is generally regarded as a target for trypsin but not for thrombin signaling. We now show that thrombin, at concentrations that can be achieved at sites of acute injury or in a tumor microenvironment, can directly activate PAR2 vasorelaxation and signaling, stimulating calcium and MAPKinase responses along with triggering beta-arrestin recruitment. Thus, PAR2 can be added alongside PARs 1 and 4 to the targets whereby thrombin can affect tissue function.

MOL #102723

INTRODUCTION

The cloning of the G-protein-coupled receptor for thrombin, which is responsible for thrombin's ability to regulate platelet function and to stimulate mitogenesis, represents a paradigm shift in understanding the general mechanism whereby proteinases regulate tissue function (Rasmussen et al., 1991; Vu et al., 1991; Hollenberg & Compton, 2002; Alexander et al., 2013: p. 1552; Adams et al., 2011; Hollenberg et al., 2014). A key finding was the discovery of the 'tethered ligand' (TL) mechanism of activation of these proteolytically activated receptors, termed 'PARs' (Vu et al., 1991; Chen et al., 1994). Thus, cleavage of the N-terminus of PAR1 by thrombin at a target arginine/serine bond unmask a tethered sequence (TL), SFLLRN---, which becomes the receptor-activating ligand (Vu et al., 1991). Similarly, thrombin cleaves an arginine-glycine bond in human PAR4 to reveal the receptor-activating TL sequence, 'GYPGQV---'. The higher potency with which thrombin activates PAR1 versus PAR4 is due to a 'hirudin-like' sequence in PAR1 that increases the affinity of thrombin for PAR1 relative to PAR4. Trypsin, known to target PAR2 at nanomolar concentrations (Nystedt et al., 1994), can also activate PAR4 with a potency equivalent to that of thrombin. However, in the human platelet, PAR3 acts as a cofactor for PAR4, to increase thrombin's potency for PAR4 activation (Nakanishi-Matsui et al., 2000). Thus, both trypsin and thrombin can regulate PAR4, whereas PAR2 is preferentially activated by trypsin but not thrombin, presumably because of a lack of a thrombin-preferred upstream proline in PAR2, just before its arginine cleavage-activation site and the lack of a hirudin-like thrombin binding domain found in PAR1. The proline residue in PARs 1 and 4 confers thrombin sensitivity to cleave the arginine and unmask the receptor-tethered ligands. Notwithstanding, human PAR2 does indeed possess potential serine proteinase cleavage sites in its N-terminal amino acid sequence at lysine residues both upstream and downstream of its arginine-36/serine-37 tethered ligand-generating site. Thus, in principle, thrombin might be able to cleave PAR2 at a basic

MOL #102723

residue to generate signaling. Indeed, thrombin activation of PAR2 has been reported, but this result has been attributed not to a direct activation of PAR2 by thrombin but rather to an indirect transactivation of PAR2 by the PAR1 tethered ligand unmasked by thrombin (O'Brien et al., 2000). For transactivation, the unmasked tethered ligand of PAR1 (SFLLR---) is thought to 'reach over' and function as an activating ligand for PAR2 (O'Brien et al., 2000; Chen et al., 1994). This mechanism presumably occurs in the setting of a PAR1/PAR2 heterodimer. For the study we report here, we hypothesized that in addition to this 'tethered ligand-crossover' mechanism involving PAR1, thrombin, at sufficiently high concentrations, can activate PAR2 directly. To test this hypothesis, we used a number of approaches, including measuring the cleavage by thrombin of a synthetic peptide representing the cleavage-activation sequence of human PAR2 and the use of a CRISPR/Cas9-targeting approach to generate a PAR1-null HEK cell line (PIN-HEK) and a PAR1-null bladder cancer cell line. These PAR1-null cells were used to evaluate the action of thrombin on cell-expressed PAR2 for signaling (calcium, MAPKinase/ERK 1/2 activation, arrestin recruitment) in the absence of PAR1. Further, we developed a new approach to evaluate PAR2 cleavage by thrombin and other proteinases by designing a PAR2 cleavage reporter assay, in which a NanoLuc luciferase tag (Nluc: Hall et al., 2012) is placed at the PAR2 N-terminus (Nluc-PAR2). Thus, cleavage of the N-terminus of Nluc-PAR2 expressed on the surface of a 'reporter cell' releases a luciferase signal into the supernatant. The Nluc tag was also placed in a mutated receptor in which the serine proteinase target arginine at the R36/S37 PAR2 cleavage-activation site was mutated to glycine: G36/S37. This G36/S37 mutant PAR2 is resistant to serine proteinase cleavage/activation. To complement the Nluc-release assay, we used a dually tagged PAR2 with an N-terminal monomer red fluorescent protein (mRFP or RFP) and a C-terminal enhanced yellow fluorescent protein (eYFP or YFP). When intact, the receptor upon imaging appears 'yellow'; but when cleaved, the loss of

MOL #102723

the N-terminal mRFP tag results in a receptor that appears ‘green’, and the released mRFP fragment is internalized as a ‘red dot’. The dynamics of receptor cleavage can be followed with confocal imaging (Ramachandran et al., 2011; Mihara et al., 2013). The thrombin-triggered interaction of PAR2 with beta-arrestins 1 and 2 was monitored using bioluminescence resonance energy transfer (BRET) between C-terminally YFP-tagged PAR2 and Renilla luciferase (rLUC)-tagged beta-arrestins as described previously (Ramachandran et al., 2011). These approaches were used to monitor the ability of thrombin to regulate PAR2 function in the PAR1-null HEK cells. Finally, we evaluated the action of thrombin to trigger a PAR2-mediated endothelium-dependent relaxation in aorta tissue derived from PAR1-null mice. Our data illustrate unequivocally that in isolation, PAR2 signaling (activation of calcium and MAPKinase signals along with beta-arrestin recruitment and vascular relaxation) can be regulated by thrombin cleavage, which we show via peptide mapping can target the N-terminal sequence of human PAR2 at its ‘canonical’ R36/S37 cleavage-activation site.

MOL #102723

MATERIALS AND METHODS

Chemicals and other reagents. PAR-selective receptor-activating peptides (TFLLR-NH₂, for PAR1; 2-furoyl-LIGRLO-NH₂ for PAR2) and the peptide sequence representing the cleavage-activation site (shown: //) of human PAR2 (SSKGR36//S37LIGKVDGTSHVTGKGVT) were prepared by solid phase synthesis by the University of Calgary Peptide Synthesis Facility (peplab@ucalgary.ca) as >95% pure products, verified by HPLC and mass spectrometry. Stock solutions of about 1 mM were prepared in 25 mM HEPES buffer, pH 7.4. Calcium ionophore (A23187) was from Sigma (St. Louis MO), and the ‘no-wash’ calcium indicator dye was from Molecular Probes (Invitrogen, Burlington, ON Canada). Thrombin from human plasma (cat# 605195; 2800 NIH U/mg) was from EMD Biosciences (San Diego, CA). Mouse monoclonal anti-phospho-p42/44 MAPK (Erk1/2) IgG (H+L) and rabbit monoclonal anti-p42/44 MAPK (Erk1/2) IgG (H+L) as well as the secondary HRP-linked anti-mouse IgG (H+L) and anti-rabbit IgG (H+L) antibodies were obtained from Cell Signaling Technology (Danvers, MA). Hybond-P PVDF membrane and ECL advanced detection kit were purchased from GE Health Healthcare Canada (Mississauga, ON, Canada). Recombinant hirudin (\approx 16,000 anti-thrombin U/mg) from Hyphen BioMed (Neuville-Sur-Oise, France) was used to neutralize thrombin by preincubation at a hirudin/thrombin molar ratio of 10:1. All other chemicals were purchased from Sigma (St. Louis, MO) unless otherwise specified.

Peptide cleavage: Cleavage of the synthetic PAR2 cleavage-activation peptide sequence (100 μ M) by thrombin (25 U/ml) was allowed to proceed for 5 to 30 min at 37 °C in 50 mM HEPES buffer pH 7.4. The reaction was terminated by the addition of two volumes of a “stop solution” (50% acetonitrile and 0.1% trifluoroacetic acid in water) to the proteolysis sample. Samples were then subjected to HPLC analysis as described previously (Oikonomopoulou et al., 2006), with

MOL #102723

collection of the E215 peak fractions, for mass spectral MALDI identification of the peptide fragments in the quantified HPLC peaks. The identity of the cleavage fragments was also deconvoluted from the masses identified in the unfractionated thrombin cleavage reaction mixture.

Cell culture. All cell media, serum, delta surface culture flasks and multiwell dishes were purchased from Thermo Fisher Scientific (Waltham, MA). HEK293 (ATCC CRL-1573) and KNRK (ATCC CRL-1569) cell lines were routinely grown in Dulbecco's minimal essential medium (DMEM) supplemented with 1 mM sodium pyruvate, 10% fetal bovine serum and 2.5 µg/ml plasmocin (Invitrogen/ThermoFisher, Carlsbad, CA) on Nunclon delta Surface Cell culture flasks at 37 °C in a 5% CO₂, humidified incubator. The cell culture procedures done routinely for the measurement of calcium signaling used enzyme-free EDTA-containing cell dissociation medium for cell passage as described in detail previously (Ramachandran et al., 2011; Mihara et al., 2013). For studies of receptor cleavage (Nluc assay) or imaging, cells were passed with enzyme-free EDTA-containing cell dissociation medium or by mild trypsinization (0.2 mL of 0.25 % trypsin-EDTA: Gibco/75 cm² T-flask) to optimize cell homogeneity on plating. After dispersal (30 sec) the trypsin was neutralized by the addition of 10% serum-containing growth medium and cells were then re-fed routinely.

Calcium signaling assay. Measurements of PAR2-stimulated calcium signaling in response to thrombin and to PAR2-selective agonists (trypsin and 2-furoyl-LIGRLO-NH₂) were conducted essentially as described previously (Kawabata et al., 1999; Ramachandran et al., 2011; Mihara et al., 2013) using a Fluo4-NW 'no wash' calcium assay kit (Thermo Fisher Scientific, Waltham, MA). PAR1-null HEK and HTB-9 cells, which express functional PAR2, were lifted from the culture flask with EDTA-supplemented calcium-free isotonic phosphate-buffered saline (pH 7.4), washed and resuspended at approximately 5×10^7 cells/ml in Hank's Buffered salt solution

MOL #102723

(HBSS) supplemented with 10 mM HEPES, 1.5 mM CaCl₂ and 1.5 mM MgCl₂ (HBSS+ buffer) containing calcium indicator dye. Agonists were added to stirred cell suspensions in a spectrofluorometer, and the fluorescence emission signal at 530 nm (excitation wavelength, 480 nm) was measured relative to the signal generated in the same cell preparation by the calcium ionophore A23187 (% A23187).

Monitoring MAPKinase-ERK 1/2 activation. Thrombin-stimulated MAPKinase-ERK 1/2 activation was monitored in KNRK cell lines expressing either PAR1 or PAR2 essentially as described previously using western blot procedures that visualize activated phospho-MAPKinase (Ramachandran et al., 2009). The PAR2-expressing KNRK cells were grown to confluence in a 24-well plate (Thermo Scientific; 2-cm² area) and serum-starved by incubation overnight in serum-free DMEM. Fresh serum-free medium was added the following day, and the cells were incubated for another 4 h. Thrombin (1 to 20 U/ml) was diluted in serum-free DMEM and was then applied to the cells at room temperature for 10 min, at which time the cells were rinsed with ice-cold buffer and processed for western blot detection of phospho-MAPKinase/ERK 1/2 (p-ERK1/2). Activation was quantified by densitometry (Image J) and expressed as a ratio of p-ERK 1/2 relative to the signal from nonstimulated cells (fold increase over baseline). Our past work has verified that the vector-transfected or nontransfected KNRK cells are unresponsive for PAR1/PAR2 activation of MAPKinase-ERK1/2.

Cloning and transfection. The plasmid encoding the human PAR2 receptor (wt-hPAR2) cloned in pCDNA3.1 was obtained from the cDNA Resource Center (Bloomsburg University, Bloomsburg, PA). A C-terminal eYFP (enhanced YFP) tag was fused in-frame with the PAR2 sequence by mutating the PAR2 stop codon to tyrosine and insertion of the eYFP fragment with flanking XhoI and XbaI restriction enzyme sites at the C-terminus of the hPAR2 coding sequence. The resulting fusion protein encodes for human PAR2 with a C-terminal eYFP tag

MOL #102723

with a short intervening XhoI linker sequence. In order to generate the dually tagged clones, restriction enzyme sites for BspEI and BamHI were created at Q27 of human PAR2 to insert the red fluorescent protein, mRFP, or the NanoLuc (Nluc) Luciferase gene fragment. The mRFP or Nluc coding PCR fragments with flanking BspEI and BamHI restriction enzyme sites were inserted in the hPAR2-eYFP cDNA. The resulting clones encoded N-terminal reporter tags with a glycine and serine linker followed by the sequence for human PAR2 and a C-terminal eYFP (NLuc-P2Y and RFP-P2Y). Mutants of the NLuc-P2Y and RFP-P2Y constructs were also prepared in which the target arginine-36 targeted by trypsin for PAR2 activation was replaced by either a glycine (R36G) or alanine (R36A). The plasmid, pNL1.1CMV, containing the Nluc gene was a gift from Promega Corporation (Madison, WI). Plasmid DNA mutations were created using the QuikChange Lightning Multi Site-Directed Mutagenesis Kit (Agilent Technologies, Mississauga, ON, Canada). All constructs were confirmed by direct sequencing (University of Calgary DNA Sequencing Facility). The functionality of wild-type and mutated Nluc-tagged PARs expressed in a KNRK cell background, that when untransfected does not respond to PAR activation, was confirmed by calcium and MAPKinase signaling measurements in response to the PAR2-activating peptide (2-furoyl-LIGRLO-NH₂). For optimal transfection of functionally active (calcium signaling) PAR2 (either dually tagged or C-terminally tagged with eYFP), HEK or HTB-9 cells were seeded into a 75-cm² T-flask and allowed to grow to about 40% confluency over approximately 6 h, at which point the expression vector was added. Transfection and growth were allowed overnight, and cells were harvested at about 70–80% confluency for calcium signaling measurements as outlined above. Allowing cells to overgrow past 80% confluency appeared to diminish their thrombin sensitivity. For imaging studies, HEK cells grown to about 25% confluency were transfected with dually-tagged PAR2. After 24 h, transfected cells were seeded into MatTek glass-bottom 24-microwell plates (1-cm diameter, MatTek Corp., Ashland,

MOL #102723

MA) coated with poly-L-lysine (100 L of 0.1 µg/ml for 1hr at room temperature; then washed) and cultured for a further 24 h. Monolayers were then re-fed with serum-containing medium supplemented with 1 µM GM6001) to reduce activation by endogenous proteinases for another 24 hrs at which time PAR2 activation, cell fixation and imaging were performed as outlined below.

Preparation of PAR1-null HEK293 and HTB-9 cells using a CRISPR approach. We used the Lenti-X 293T cell line (Clontech, Mountain View, CA), which constitutively expresses functional PARs 1 and 2 (Kawabata et al., 1999), to generate HEK and HTB-9 cell lines devoid of PAR1 employing a CRISPR/Cas9 approach. ATCC®-HTB-9™ cells originating from ATTC, which we validated to respond (calcium signaling) to both PAR1 and PAR2 activation, were kindly provided by Dr. Andries Zjilstra, Vanderbilt University. The knock out design and procedures used to derive the PAR1-null cells from the wild-type HEK and HTB-9 cells were as described by Zhang and colleagues (Sanjana et al., 2014; Shalem et al., 2014) using the GEKO CRISPR protocol (<https://www.addgene.org/crispr/libraries/geckov2/>). Three sets of genome-specific sgRNA sequences of PAR1 (F2R) were chosen from the GeCKOv2 Human Library, and we synthesized both strands of oligo nucleotides for each target sequence (F2R, HGLibA_15861_F: caccgGATAGACACATAACAGACCG, R: aaacCGGTCTGTTATGTGTCTATCC; F2R, HGLibA_15862_F: caccgCTCAATGAAACCCTGCTCGA, R: aaacTCGAGCAGGGTTTCATTGAGC; F2R, HGLibA_15861_F: caccgAGCCCGGGACAATGGGGCCG, R: aaacCGGCCCCATTGTCCCGGGCTC). Here, the upper case sequences are target sequences of the PAR1 genomic locus and the lower case sequences are flanking sequences for cloning. Both strands of the oligonucleotides were annealed and inserted in BsmBI restriction enzyme sites

MOL #102723

under a U6 promoter in a CRISPR/CAS9 vector, lentiCRISPR v2, a gift from Feng Zhang (Addgene plasmid # 52961).

The lentiCRISPR v2 plasmids containing three PAR1-targeting sequences were mixed and transfected using Lipofectamine® LTX Reagent. The transfected cells were maintained in the presence of 5 µg/ml puromycin to select knockout cells. The absence of functional PAR1 in the PAR1-null Lenti-X 293T cells (P1Null-HEK) and the PAR1-null HTB-9 cells was verified using a calcium signaling assay (Kawabata et al., 1999; Mihara et al., 2013) in which no signal was observed for either thrombin or the PAR1-activating peptide, TFLLR-NH₂, in cells that were otherwise responsive to the PAR2-activating peptide, 2fLI (Figure 3, tracing B). Further, the PAR1-null cells derived in this way became PAR1-responsive when reconstituted with wild-type PAR1. The Lenti-X 293T clone (P1Null-HEK) and a clone of PAR1-null HTB-9 cells were then used as background cells to interrogate the impact of thrombin action on PAR2, which was expressed either constitutively in the cells (HTB-9) or which was supplemented (HEK cells) by transiently transfecting into the cells wild-type PAR2 either with a C-terminal eYFP (Ramachandran et al., 2009) or as a dual-tagged receptor bearing an N-terminal mRFP and a C-terminal YFP: RFP-PAR2-YFP. The PAR2-expressing PAR1-null cells (P1N-HEK/PAR2-Y; P1N-HTB9) were then used to evaluate the ability of thrombin to regulate PAR2.

PAR cleaving activity monitored by an Nluc release assay. We developed a new assay to detect the proteolytic cleavage of the N-terminus of PAR2 by enzymes that can target either the cleavage-activation site or other extracellular locations. Our approach involves placing an N-terminal NanoLuc luciferase (Nluc) tag (Hall et al., 2012) on PAR2 that also has a C-terminal eYFP tag to monitor receptor expression (Nluc-PAR2-eYFP). Thus, our method can assess the PAR-cleaving activity of either a specific proteinase or any proteolytic enzyme present in body fluids or secreted by cells into a culture medium. For our work, we sought an ‘indicator cell’ in

MOL #102723

which the Nluc-tagged PAR2 could be expressed in the absence of cell-secreted proteinases. To this end, we selected a human embryonic lung fibroblast cell line transformed with SV40, WI-38 VA-13 2RA (WI38VA13), as a transfected Nluc-PAR2-eYFP-expressing ‘indicator cell’, which is similar to a normal fibroblast phenotype and which we found secretes minimal PAR-cleaving proteinases. The Nluc-hPAR2-eYFP plasmid DNA was transfected into the WI-38 VA-13 cells with FuGENE HD (Promega) and selected with 300 µg/ml G418. The Nluc-PAR1-YFP-expressing cells, WI38(NlucPAR2), were further selected by flow cytometry (Flow Cytometry Core Facility, University of Calgary, Health Sciences Centre) by monitoring fluorescence from the C-terminal PAR2 eYFP.

The Nluc release assay to detect PAR-cleaving proteolytic activity was performed using 24-well (1-cm diameter) plates as follows. Confluent WI38 (NlucPAR2) cells in a T75 flask were first washed three times with 1 ml of isotonic Dulbecco’s calcium-magnesium-free phosphate-buffered saline, pH 7.4 (PBS)-1 mM EDTA. Ten minutes after the last wash and incubation of the monolayer at 37 °C in the residual buffer adhering to the monolayer, approximately 200–240 µl (4 drops with a polyethylene transfer pipette) of 0.05% (w/v) trypsin in PBS-1 mM EDTA was added to the washed monolayer and allowed to incubate for 3 min at room temperature to ensure disaggregation of the cells (the final trypsin concentration was approximately 0.025% w/v). Cells were then suspended in 18 ml of culture medium (DMEM/10% fetal bovine serum) to neutralize the trypsin. Aliquots of the cell suspension (500 µl) were then added into each well of a 24-well (1-cm diameter) plate and cultured for approximately 48 h. The cell monolayers were then washed three times with HBSS, pH 7.4, and 100 µl of 10 mM HEPES, pH 7.4-supplemented HBSS containing 1.5 mM each of MgCl₂ and CaCl₂ (HBSS+) was added to each well. The test amount of proteinase in a final volume of 100 µl of HBSS+ was then added to the Nluc-expressing cell monolayers (final volume, 200 µl) and incubated for 30 min at room temperature,

MOL #102723

at which time aliquots of the supernatant (100 μ l) were withdrawn to measure released Nluc activity. Aliquots from three replicate samples for each enzyme concentration were transferred to a white 96-multiwell black plate followed by the addition of diluted luciferase assay substrate solution. The substrate solution supplied with the Nano-Glo Luciferase Assay kit was diluted 10-fold with HBSS+ buffer, and 20 μ l of this diluted substrate solution was added to 100 μ l of cell supernatant. Luminescence from the luciferase activity, which stabilized between 5 and 60 min, was measured using a Victor X4 plate reader (PerkinElmer Life Sciences), according to the manufacturer's instructions. The luminescence yield was approximately linear between approximately 0.5 to 10 BAEE U/ml trypsin activity. For concentration-effect curves measuring the ability of thrombin and trypsin to cleave/release the N-terminal Nluc reporter, data were normalized for each enzyme concentration relative to the background luminescence observed in the absence of enzyme (% luminescence). Work was done with both wild-type Nluc-tagged PAR2 and with an Nluc-tagged PAR2 having an R36G mutation that prevents cleavage and unmasking of the PAR2 tethered ligand sequence by trypsin or other serine proteinases. On average, the maximum increase in luminescence over background of was from 4,500 to 27,400 and 2,100 to 2,300 luminescence counts/0.1 sec/sample for wild type and mutant PAR2 by thrombin cleavage, compared with 1,400 to 31,000 and 500 to 2,900 luminescence counts/0.1 sec/sample for wild type and mutant PAR2 by trypsin.

Imaging cleavage/activation of dual-labeled PAR2. Cleavage of the N-terminal domain of PAR2 expressed in an HEK cell background, cultured for imaging experiments as described above, was monitored by confocal imaging using N-terminal mRFP and C-terminal eYFP dually tagged PAR2 (RFP-PAR2Y) either without or with an alanine for arginine substitution at residue 36 (R36A: RFP-PAR2Y-R/A) to eliminate the tethered ligand site cleaved by thrombin. Monolayers that had grown for 24 h in the MMP-inhibitor-containing medium were washed three

MOL #102723

times with DMEM, and PAR2 activation was triggered by the addition of either enzyme (trypsin, 2–5 U/ml; thrombin, 25–50 U/ml) or PAR2-activating peptide (2 μ M fLIGRLO-NH₂) to the cell supernatant. Receptor activation was stopped at timed intervals by the addition of 1 ml of 10.5% formalin fixative (BDH Chemicals/VWR Edmonton AB) to the 0.2 ml of cell supernatant. Upon confocal imaging, intact PAR2 appears yellow, combining the red from the N-terminal mRFP and artificial green from the C-terminal eYFP. After cleavage/activation by thrombin, the N-terminal mRFP is released and PAR2 appears green due to the C-terminal eYFP tag.

Measurement of bioluminescence resonance energy transfer (BRET) between PAR2-eYFP and arrestins 1 and 2. Measurements of BRET between C-terminal eYFP tagged PAR2 and Renilla reniformis luciferase-tagged beta-arrestins 1 and 2 were measured as described by us previously (Ramachandran et al., 2009; Ramachandran et al., 2011; Mihara et al., 2013), with luminescence values measured at 20 min. after receptor activation, in keeping with the procedure described by Hamdan et al., (2005).

Measurements of PAR-induced endothelium-dependent vascular relaxation. Endothelium-dependent vasorelaxation was measured as described previously (McGuire et al., 2002) using isolated mouse aorta rings obtained from PAR1-null mice used by us in previous studies of PAR function (Cenac et al., 2005). Tissues with a verified endothelium-dependent relaxant response to acetylcholine were constricted with phenylephrine (2.5 μ M), and a relaxant response to thrombin (5 to 50 U/ml) or a PAR2-activating peptide (2-furoyl-LIGRLO-NH₂) was monitored. The response was measured in the absence and presence of a 10-fold molar excess thrombin-inhibitory concentration of hirudin. The thrombin response was also measured (10 U/ml) after first desensitizing the vascular endothelial response by repeated exposure to the PAR2-activating peptide, 2fLIGRLO-NH₂ (2 \times 5 μ M).

MOL #102723

RESULTS AND DISCUSSION

Thrombin cleavage of a synthetic peptide derived from the N-terminal PAR2 tethered ligand sequence. We first established that thrombin can cleave a synthetic peptide derived from the N-terminal human PAR2 that contains the ‘canonical’ PAR2 tethered ligand sequence unmasked by trypsin (GTNRSSKGR//**SLIGKVDGTSHVTGKGVT**: trypsin cleavage site denoted by//; tethered ligand sequence in bold red letters). As illustrated in Figure 1, thrombin (25 U/ml) can indeed cleave the synthetic PAR2-derived N-terminal peptide to unmask the receptor-activating tethered ligand sequence, ‘SLIGKV--’. Of note, although not identified as a distinct peak in the HPLC analysis, deconvolution of the peptide masses detected by MALDI mass spectral analysis of the cleavage reaction mixture provided evidence for the presence of the peptide SSKGRSLIGKVDGTSHVTGKGVT. That peptide would originate from an upstream cleavage of the PAR2 sequence: GTNR//SSKGR**SLIGKVDGTSHVTGKGVT**. The next issue to deal with was to verify that thrombin is able to cleave the N-terminal sequence of PAR2 when expressed in an intact cell system.

Thrombin cleavage/release of luciferase activity from the Nluc-tagged-PAR2 N-terminus. We monitored the ability of thrombin to cleave the PAR2 N-terminus, as indicated by the release of the N-terminal Nluc tag from PAR2 expressed in WI38VA13 cells (scheme shown in panel A of Figure 2). As shown in the middle and right panels of Figure 2, thrombin, like trypsin (2–50 U/ml of each enzyme), was able to release the N-terminus of PAR2 from the cell surface to yield a luciferase signal in the supernatant. Thrombin was also able to cleave/release the PAR2 N-terminal domain when the receptor was expressed in several other cell backgrounds (e.g. CHO: data not shown). Significantly, the Nluc-PAR2 clone with an R36G mutation at the trypsin cleavage-activation site, which is no longer a tryptic substrate, did not release luciferase activity when treated with either trypsin or thrombin at concentrations of up to 2 U/ml trypsin and 50

MOL #102723

U/ml thrombin activity (dashed lines, Figs. 2B and 2C). Given that thrombin appeared to cleave the N-terminus of PAR2 at the same arginine-36 as trypsin, the next issue was to determine if the cleavage resulted in receptor activation.

Activation of PAR2 by thrombin to stimulate calcium and MAPKinase signaling along with beta-arrestin interactions. Since previous publications indicate that PAR1 and PAR2 can cooperate for cell signaling, possibly as a heterodimer, we wished to use cells in which PAR2 can signal in the absence of PAR1. Therefore, as done in previous work (Al-Ani et al., 2004), we used PAR2-transfected KNRK cells that as a wild-type cell do not express either functional PAR1 or PAR2 and that as transfected cells express functional PARs. Further, we used an HEK293 background cell line that constitutively expresses functional PARs 1 and 2 (Kawabata et al., 1999) to prepare a PAR1-null HEK cell line (P1N-HEK) with a CRISPR/Cas9 approach. The PAR1-null HEK cells were also used as transient transfection targets for the expression of either PAR2 with a C-terminal eYFP tag or dually tagged PAR2, having an N-terminal RFP tag and a C-terminal eYFP. In the PAR1-null HEK cell background, these tagged PAR2 constructs were used to monitor: 1. PAR2-mediated calcium signaling activated by thrombin, trypsin or a PAR2-activating peptide, 2. Interactions of activated PAR2 with beta-arrestins 1 and 2, as described previously (Ramachandran et al., 2011) and 3. Receptor cleavage and post-activation dynamics, as done previously for PAR1 (Mihara et al., 2013). The PAR2-expressing KNRK cells were used to monitor PAR2-mediated MAPKinase signaling triggered by thrombin, in keeping with work done with these PAR2-expressing cells in the past (Ramachandran et al., 1999).

Calcium signaling. As shown in Tracing A of the left panel of Figure 3, the wild-type Lenti-X 293T cells (WT-HEK), from which the PAR1-null HEK line was derived, generated a prominent calcium signal when stimulated by either the PAR1-selective agonist, TFLLR-NH₂, or the PAR2-selective agonist, 2-furoyl-LIGRLO-NH₂. Further, a calcium signal was stimulated by

MOL #102723

either thrombin (via PAR1) or trypsin (via PAR2) in the wild-type HEK 293T cells that had first been cross-desensitized by pretreatment with the selective PAR1 agonist (TFLLR-NH₂) to enable activation of PAR2 only; or desensitization with the selective PAR2 agonist (2-furoyl-LIGRLO-NH₂) to measure only PAR1 activation. Thus, thrombin yielded a PAR1 calcium signal in the PAR2-desensitized cells; and trypsin likewise yielded a PAR2 signal in the PAR1-desensitized cells. In contrast, at concentrations that activated PAR1 in the wild-type HEK293 cells, neither the PAR1-activating peptide, TFLLR-NH₂ (10 to 25 μ M), nor thrombin (25 to 50 U/ml) was able to generate a calcium signal in the PAR1-null HEK cells, whereas the cells were fully responsive to PAR2 activation either by the PAR2-activating peptide, 2-furoyl-LIGRLO-NH₂, or by trypsin (Tracing B, left-hand panel of Figure 3). However, when the PAR1-null HEK cells were transiently transfected with dual-tagged PAR2 to increase the abundance of PAR2 expression, thrombin was able to stimulate a calcium signal that was about 40% of the magnitude of the signal triggered by trypsin (Tracing C, left-hand panel of Figure 3). In the same PAR1-null HEK cells in which PAR2 was desensitized, the PAR1-activating peptide, TFLLR-NH₂, did not generate a signal, as expected (first portion of Tracing C, left panel of Figure 3). Further, the signal generated by 10 to 50 U/ml thrombin was neutralized by preincubation of thrombin with a 10-fold molar excess of hirudin (Figure 3, Tracing E); and the addition of 1 μ g/ml of soybean trypsin inhibitor (STI) was without effect on the thrombin-stimulated calcium signal, whereas STI completely abrogated the signal caused by 0.5 U/ml trypsin (data not shown). Finally, the desensitization of the PAR2 response in the PAR1-null HEK cells expressing the PAR2-Y receptor by repeated exposure to the PAR2 agonist 2fLIGRLO-NH₂ eliminated the response to thrombin (Figure 3, tracing F). We concluded that the signal generated by our thrombin preparation reflected PAR2 activation and was indeed due to thrombin itself and not to a contaminating trypsin-like enzyme.

MOL #102723

Of note, when the PAR1-null HEK cells were transfected with the R36A PAR2 mutant (P1N-HEK/PAR2-Y-R/A), in which the thrombin cleavage site identified by HPLC analysis was no longer a tryptic target, the calcium signal generated by thrombin was absent (Tracing D, Figure 3), although the PAR2-activating peptide, which acts independently of the tethered ligand, was still able to trigger a calcium signal (second response from the left, Tracing D, left-hand panel of Figure 3). That result demonstrated the presence of ample functional R36A-PAR2 in the cells that was resistant to enzyme cleavage-activation but not to activation by the PAR2-activating peptide (Tracing D, Figure 3). Thus, thrombin yielded a PAR2 signal in the PAR1-null HEK cells only when transfected with a PAR2 construct with a susceptible tryptic cleavage site at arginine-36.

To validate the data obtained with the PAR1-null HEK cells, we generated a PAR1-null bladder carcinoma-derived HTB-9 cell line. In the wild-type HTB-9 cells, both PAR1 and PAR2 agonists caused calcium signals equivalent to those observed for the wild-type HEK cells (comparable to the responses in tracing A, Figure 3). Similar to the PAR1-null HEK cells, the PAR1-null HTB-9 cells did not respond to PAR1 activation by the PAR1-activating peptide, TFLLR-NH₂ (not shown). However, the nontransfected PAR1-null HTB-9 cells, like the PAR1-transfected PAR1-null HEK cells, did indeed yield a calcium signaling response to thrombin in the concentration range of 25–50 U/ml (concentration-response curves for HEK and HTB-9 cells: Figure 3, right panel G). The greater thrombin sensitivity of the transfected PAR1-null HEK cells relative to the HTB-9 cells (lower EC₅₀ for HEK cells: Panel G, Figure 3) was presumably due to the lower abundance of PAR2 expression in the HTB-9 cells. The data thus verified unequivocally that thrombin can activate PAR2 calcium signaling in both the PAR1-null HEK and PAR1-null HTB-9 cells that express functional PAR2. Thus, thrombin at sufficiently high concentrations can in

MOL #102723

principle signal via both PAR1 and PAR2 using both a direct cleavage mechanism as well as an indirect (i.e. tethered ligand crossover) mechanism for PAR2 activation.

Vascular action of thrombin via PAR2 in PAR1-null mice. To evaluate the potential impact of thrombin to activate endothelial PAR2 *in vivo*, we measured the endothelium-dependent relaxant activity of thrombin in a PAR2-responsive aorta tissue preparation derived from PAR1-null mice (Figure 3, right Panel G). The relaxant response of the aorta preparation from the PAR1-null animals due to PAR2 activation was abrogated both by pre-desensitization of the PAR2 relaxant response with repeated exposure to the PAR2 agonist 2-furoyl-LIGRLO-NH₂ (second tracing on the right, Panel H, Figure 3) and by neutralizing the thrombin preparation with a 10-fold molar excess of hirudin (not shown). Further, the addition of 1 µg/ml soya trypsin inhibitor did not affect the thrombin-mediated relaxant response, but completely blocked the response to 0.5 U/ml trypsin (not shown). The results with the enzyme-selective inhibitors of thrombin and trypsin verified that the relaxation was generated by thrombin and not by a contaminating trypsin-like enzyme. Our data thus showed that thrombin is capable of causing PAR2 activation in intact vascular tissues *in vivo*, albeit at relatively high concentrations relative to those that cause coagulation.

MAPKinase-ERK 1/2 activation. In addition to stimulating PAR2 calcium signaling in the PAR1-null HEK cells, thrombin also stimulated MAPKinase-ERK 1/2 signaling in the PAR2-expressing KNRK cells (Figure 4). The phospho-MAPKinase signal caused by 2 to 20 U/ml thrombin in the PAR2-expressing KNRK cells (left western blot, Panel A) was comparable to the signal generated by 1 U/ml thrombin in the PAR1-expressing KNRK cells (right western blot, Panel A). The densitometrically quantified concentration dependence of thrombin-mediated PAR2 activation is shown in the lower panel B of Figure 4.

MOL #102723

Thrombin-stimulated PAR2-arrestin interactions. Using the PAR1-null HEK cells expressing N-RFP/C-YFP-tagged PAR2, we next evaluated the ability of thrombin to drive PAR2-arrestin interactions. As shown in Figure 5, thrombin-mediated activation of PAR2 promoted interaction of the receptor with both arrestins 1 and 2. We thus concluded that at concentrations in the range of 10 to 25 U/ml (100 to 250 nM), thrombin can stimulate PAR2 calcium and MAPKinase signaling along with beta-arrestin interactions.

Visualizing thrombin-triggered PAR2 cleavage-activation. Finally, we wished to visualize PAR2 cleavage-activation by thrombin using confocal microscopy. As shown in Panel 2 of Figure 6, thrombin cleavage released the N-terminal mRFP tag from PAR2, which results in the receptor image appearing 'green' along with the vesiculation and internalization of the receptor. Trypsin activation triggered the same response (not shown). In contrast the receptor with the cleavage-resistant R36A mutation at the tryptic cleavage/activation site was resistant to thrombin cleavage and the receptor remained 'yellow' (Panel 4, Figure 6). In separate experiments, we verified that activation of the C-terminally YFP-tagged receptors by trypsin, as for the dually tagged receptor, caused internalization (not shown). Further, the PAR2-activating peptide, 2fLI, also triggered internalization of both the dually-tagged wild-type and thrombin-resistant R/A mutant receptor (not shown).

Summing up. We have demonstrated the ability of thrombin to activate PAR2 directly, using a number of independent approaches, including: 1. Cleavage of the N-terminal synthetic peptide sequence of PAR2 *in vitro*, 2. Monitoring PAR2 N-terminal cleavage and release from the cell surface using a new Nluc release assay, 3. Measuring thrombin-mediated PAR2 calcium and MAPKinase signaling, along with beta-arrestin interactions in cells lacking the expression of functional PAR1 and PAR4, 4. Visualizing thrombin-mediated PAR2 cleavage using dually

MOL #102723

tagged N-RFP-C-YFP PAR2 receptors expressed in HEK cells and 5. Demonstrating thrombin-triggered PAR2-mediated vasorelaxation in PAR1-null vascular tissue. That said, we found that thrombin-mediated activation of PAR2, including PAR2-mediated vasorelaxation in intact vessels, occurs only at concentrations of the enzyme (10 to 50 U/ml; 100 to 500 nM) that are much higher than those that regulate platelet function *in vivo* or that stimulate PAR1 signaling in our background HEK and HTB-9 cells *in vitro* (0.5 to 5 U/ml; 5 to 50 nM; Mihara et al., 2013). Although our data fully support our hypothesis that thrombin at sufficiently high concentrations can activate PAR2 directly, the question is: Can this action of thrombin play a physiological role? We suggest that the answer to this question is ‘yes’, but only in unique situations such as in a tumor microenvironment or in the setting of acute tissue trauma where high levels of active thrombin can be generated. Thus, since the circulating concentration of prothrombin in normal subjects ranges from 700 nM to 1.7 μ M (Henderson et al., 1980), its conversion to thrombin in an acute setting could indeed reach the levels we find can activate PAR2. In fact, unusually high levels of acutely generated thrombin have been found *in vivo* in cancer patients. In a study of 1033 patients with malignancies of the breast, lung, gastrointestinal tract, pancreas, kidney, prostate, or brain or having lymphoma, multiple myeloma, or other tumor types, the median peak thrombin concentration was found to be 500 nM (Ay et al., 2011). Similarly, breast cancer patients have demonstrated significantly higher levels of thrombin generation than controls, reaching levels of greater than 500 nM (Chaari et al., 2014). Moreover, in a study of blunt trauma patients, the range of peak thrombin in the injured individuals was nearly 30 times that of controls; and the patients with the most severe injury had thrombin levels of 300 nM (Park et al., 2012). Thus, thrombin concentrations that we have shown can activate PAR2 can indeed be found *in vivo*.

MOL #102723

In addition, although PAR1 and PAR2 are often co-expressed in a cellular setting, there are situations in which PAR2 may be expressed in the absence of PAR1. In that circumstance, the ability of an activated thrombin receptor to transactivate PAR2 would not be possible; and therefore a direct activation of PAR2 by thrombin would be of physiological significance. Thus, our data indicate that one can add PAR2 to the list of thrombin targets that can potentially regulate cell signaling in addition to PARs 1 and 4. The impact of this action of thrombin, which we propose is feasible in a restricted environment where a substantial fraction of circulating prothrombin is activated (e.g., in a tumor microenvironment), remains to be established *in vivo*.

MOL #102723

ACKNOWLEDGEMENTS

The imaging data we report could not have been obtained without the full support of the University of Calgary Cumming School of Medicine Snyder Institute's Live Cell Imaging Facility under the direction of Dr. Pina Colorusso. We are indebted to Dr. May Ho who generously provided the hirudin for our studies along with advice for its use to neutralize thrombin's activity and to Dr. Andries Zijlstra for providing us with the HTB-9 cells. We are grateful to Johnson & Johnson Pharmaceutical Research & Development for the provision of the PAR1-null mice used for our work.

MOL #102723

AUTHORSHIP CONTRIBUTIONS IN ALPHABETICAL ORDER

Participated in research design: Gibson, Hansen, Hollenberg, Mihara, Polley, Ramachandran, Renaux, Saifeddine

Conducted experiments: Gibson, Mihara, Polley, Ramachandran, Renaux, Saifeddine, Vanderboor.

Contributed new reagents or analytic tools: not applicable

Performed data analysis: Hollenberg, Gibson, Mihara, Polley, Ramachandran, Renaux, Vanderboor

Wrote or contributed to the writing of the manuscript: Hansen, Hollenberg, Mihara, Ramachandran

MOL #102723

REFERENCES

Adams MN, Ramachandran R, Yau MK, Suen JY, Fairlie DP, Hollenberg MD and Hooper JD (2011) Structure, function and pathophysiology of protease activated receptors. *Pharmacol Ther* **130**: 248-282.

Al-Ani B, Hansen KK, Hollenberg MD (2004) Proteinase-activated receptor-2: key role of amino-terminal dipeptide residues of the tethered ligand for receptor activation. *Mol Pharmacol* **65**: 149-156.

Alexander SP, Benson HE, Faccenda E, Pawson AJ, Sharman JL, Spedding M, Peters JA, Harmar AJ and Collaborators C (2013) The Concise Guide to Pharmacology 2013/14: G protein-coupled receptors *Br J Pharmacol* **170**: 1459-1581.

Ay C, Dunkler D, Simanek R, Thaler J, Koder S, Marosi C, Zielinski C, Pabinger I (2011) Prediction of venous thromboembolism in patients with cancer by measuring thrombin generation: results from the Vienna Cancer and Thrombosis Study. *J Clin Oncol* **29**: 2099-2103.

Cenac N, Cellars L, Steinhoff M, Andrade-Gordon P, Hollenberg MD, Wallace JL, Fiorucci S, Vergnolle N (2005) Proteinase-activated receptor-1 is an anti-inflammatory signal for colitis mediated by a type 2 immune response. *Inflamm Bowel Dis*. **11**:792-798.

Chaari M, Ayadi I, Rousseau A, Lefkou E, Van Dreden P, Sidibe F, Ketatni H, Galea V, Khaterchi A, Bouzguenda R, Frikha M, Ghorbal L, Daoud J, Kallel C, Quinn M, Gligorov J, Lotz JP, Hatmi M, Elalamy I, and Gerotziafas GT (2014) Impact of breast cancer stage, time from diagnosis and chemotherapy on plasma and cellular biomarkers of hypercoagulability. *BMC Cancer* **14**: 991-1003.

Chen J, Ishii M, Wang L, Ishii K, Coughlin SR (1994) Thrombin receptor activation. Confirmation of the intramolecular tethered liganding hypothesis and discovery of an alternative intermolecular liganding mode. *J Biol Chem* **269**: 16041-16045.

MOL #102723

Coughlin, SR (2005). Protease-activated receptors in hemostasis, thrombosis and vascular biology. *J Thromb Haemost* **3**: 1800-1814.

Hall, M. P., Unch, J., Binkowski, B. F., Valley, M. P., Butler, B. L., Wood, M. G., Otto, P., Zimmerman, K., Vidugiris, G., Machleidt, T., Robers, M. B., Benink, H. A., Eggers, C. T., Slater, M. R., Meisenheimer, P. L., Klaubert, D. H., Fan, F., Encell, L. P., and Wood, K. V. (2012) Engineered luciferase reporter from a deep sea shrimp utilizing a novel imidazopyrazinone substrate. *ACS Chem. Biol* **7**: 1848-1857.

Hamdan FF, Audet M, Garneau P, Pelletier J, and Bouvier M (2005) High throughput screening of G protein-coupled receptor antagonists using a bioluminescence resonance energy transfer 1-based beta-arrestin2 recruitment assay. *J Biomol Screen* **10**: 463–475.

Henderson JM, Stein SF, Kutner M, Wiles MB, Ansley JD, Rudman D (1980) Analysis of Twenty-three plasma proteins in ascites. The depletion of fibrinogen and plasminogen. *Ann Surg* **192**: 738-742.

Hollenberg, MD. & Compton, SJ (2002) International Union of Pharmacology. XXVIII. Proteinase-activated receptors. *Pharmacol Rev* **54**: 203-217.

Hollenberg MD, Mihara K, Polley D, Suen JY, Han A, Fairlie DP, Ramachandran R (2014) Biased signalling and proteinase-activated receptors (PARs): targeting inflammatory disease. *Br J Pharmacol* **171**: 1180-1194.

Ishihara H, Connolly AJ, Zeng D, Kahn ML, Zheng YW, Timmons C, Tram T & Coughlin SR (1997) Protease-activated receptor 3 is a second thrombin receptor in humans. *Nature* **386**: 502-506.

Kawabata A, Saifeddine M, Al-Ani B, Leblond L, Hollenberg MD (1999) Evaluation of proteinase-activated receptor-1 (PAR1) agonists and antagonists using a cultured cell receptor

MOL #102723

desensitization assay: activation of PAR2 by PAR1-targeted ligands. *J Pharmacol Exp Ther* **288**: 358-570.

McGuire JJ, Hollenberg MD, Andrade-Gordon P and Triggle CR (2002) Multiple mechanisms of vascular smooth muscle relaxation by the activation of proteinase-activated receptor 2 in mouse mesenteric arterioles. *Br J Pharmacol.* **135**:155-169.

Mihara K, Ramachandran R, Renaux B, Saifeddine M and Hollenberg MD (2013) Neutrophil elastase and proteinase-3 trigger G protein-biased signaling through proteinase-activated receptor-1 (PAR1) *J Biol Chem* **288**: 32979-32990.

Nakanishi-Matsui M, Zheng YW, Sulciner DJ, Weiss EJ, Ludeman MJ & Coughlin, SR (2000) PAR3 is a cofactor for PAR4 activation by thrombin. *Nature*, **404**: 609-13.

O'Brien PJ, Prevost N, Molino M, Hollinger MK, Woolkalis MJ, Woulfe DS, Brass LF (2000) Thrombin responses in human endothelial cells. Contributions from receptors other than PAR1 include the transactivation of PAR2 by thrombin-cleaved PAR1. *J Biol Chem* **275**: 13502-13509.

Oikonomopoulou K, Hansen KK, Saifeddine M, Tea I, Blaber M, Blaber SI, Scarisbrick I, Andrade-Gordon P, Cottrell GS, Bunnett NW, Diamandis EP, Hollenberg MD (2006) Proteinase-activated receptors, targets for kallikrein signaling. *J Biol Chem* **281**: 32095-32112.

Park MS1, Owen BA, Ballinger BA, Sarr MG, Schiller HJ, Zietlow SP, Jenkins DH, Ereth MH, Owen WG, Heit JA (2012) Quantification of hypercoagulable state after blunt trauma: microparticle and thrombin generation are increased relative to injury severity, while standard markers are not. *Surgery* **151**: 831-836. PMID 22316436.

Ramachandran R, Mihara K, Chung H, Renaux B, Lau CS, Muruve DA, DeFea KA, Bouvier M, Hollenberg MD (2011) Neutrophil elastase acts as a biased agonist for proteinase-activated receptor-2 (PAR2). *J Biol Chem* **286**: 24638-24648.

MOL #102723

Ramachandran R, Mihara K, Mathur M, Rochdi MD, Bouvier M, Defea K, Hollenberg MD (2009) Agonist-biased signaling via proteinase activated receptor-2: differential activation of calcium and mitogen-activated protein kinase pathways. *Mol Pharmacol* **76**: 791-801.

Rasmussen UB, Vouret-Craviari V, Jallat S, Schlesinger Y, Pages G, Pavirani A, Lecocq JP, Pouyssegur J and Van Obberghen-Schilling E (1991) cDNA cloning and expression of a hamster alpha-thrombin receptor coupled to Ca²⁺ mobilization. *FEBS Lett* **288**:123-128.

Sanjana NE, Shalem O, Zhang F (2014) Improved vectors and genome-wide libraries for CRISPR screening. *Nat Methods*. 11(8):783-784.

Shalem O, Sanjana NE, Hartenian E, Shi X, Scott DA, Mikkelsen TS, Heckl D, Ebert BL, Root DE, Doench JG, Zhang F (2014) Genome-scale CRISPR-Cas9 knockout screening in human cells. *Science*. 343:84-87.

Vu TK, Hung DT, Wheaton VI and Coughlin SR (1991) Molecular cloning of a functional thrombin receptor reveals a novel proteolytic mechanism of receptor activation. *Cell* **64**: 1057-1068.

MOL #102723

FOOTNOTES

These studies were supported in large part by an operating grant from the Canadian Institutes of Health Research (MDH), with ancillary funding from Prostate Cancer Canada, The Calgary Prostate Cancer Centre and the Calgary Motorcycle Ride for Dad. Over part of the time-frame of these studies, KKH and RR were supported in part by post-doctoral fellowships from the Alberta Heritage Foundation for Medical Research (now: Alberta Innovates Health Solutions).

Reprint requests:

Morley D. Hollenberg

University of Calgary Cumming School of Medicine

3330 Hospital Drive NW

Calgary AB Canada T2N 4N1

email: mhollenb@ucalgary.ca

MOL #102723

FIGURE LEGENDS

Figure 1: Thrombin-mediated cleavage of the PAR2-derived synthetic N-terminal ‘tethered ligand’-containing peptide sequence, SSKGR//SLIGKVDGTSHVTGKGV**T (tethered ligand sequence unmasked by cleavage (//) shown in red font).** The synthetic peptide (100 μ M) representing the N-terminal cleavage-activation domain of PAR2 was subjected to thrombin cleavage (25 U/ml) and HPLC analysis followed by MALDI mass spectral identification of the peptide fragments as described in Materials and Methods.

Figure 2: Thrombin cleavage-release of the PAR2 N-terminal domain from Nluc-tagged PAR2. A (left). The scheme illustrates the mechanism whereby thrombin cleavage of the N-terminus of PAR2 releases NanoLuc luciferase (Nluc) into the cell supernatant as an index of receptor cleavage. **B & C (middle and right).** Concentration-effect curves for the cleavage/release of the N-terminal domain of PAR2 by increasing concentrations of either thrombin (NIH U/ml) (**B**) or trypsin (BAEE U/ml) (**C**). Cleavage of the wild-type PAR2 sequence (solid line) is compared to cleavage of the R36G mutant (dashed line), which is resistant to serine proteinase cleavage. Values (% luminescence, relative to control untreated monolayer values) represent the mean values \pm s.e.m. (bars) for three replicates within an individual NLuc cleavage assay. Baseline absolute luminescence values ranged from 1400 (trypsin) to 4500 (thrombin) luminescence units for wild type PAR2 and 455 (trypsin) to 2000 (thrombin) luminescence units for the R/A mutant PAR2 and maximal values were from 36,000 (trypsin, 50 U/ml) to 27,000 units (thrombin, 50 U/ml) for wild type PAR2.

Figure 3: Thrombin-mediated calcium signaling via PAR2 (P1N-HEK/PAR2-Y; P1N-HTB-9 cells), but not the cleavage-resistant PAR2 mutant (P1N-HEK/P2Y-R/A) expressed in PAR1-null HEK cells (P1N-HEK) and vascular relaxant action of thrombin via PAR2 in

MOL #102723

PAR1-null aorta tissue. LEFT PANEL, A to F: Tracing A: Wild-type HEK cells respond (calcium signaling: Upward deflection, Tracing A) to PAR1 and PAR2 activation by either enzyme [Thrombin (1 U/ml Thr, ▲) for PAR1; trypsin (5 U/ml Trp ▽) for PAR2 or by the PAR-selective activating peptides [TFLLR-NH₂: ○, 10 μM TF for PAR1; 2-furoyl-LIGRLO-NH₂, ■, 1 μM 2fLI for PAR2]. **Tracing B:** PAR1-null HEK cells (P1N-HEK) no longer respond to activation by either the PAR1-activating peptide (○, 10–25 μM TF) or thrombin (▲, Thr, 25–50 U/ml). **Tracing C:** PAR1-null HEK cells transfected with wild-type, YFP-labeled PAR2 (P1N-HEK/PAR2-Y) respond to 2-furoyl-LIGRLO-NH₂ (■, 1 μM) and thrombin (Thr: ▲, 25 U/ml), but not to the PAR1-activating peptide (○, 10–25 μM TF) added after the cells were first desensitized with 2fLI to eliminate TF-mediated PAR2 signaling. **Tracing D:** PAR1-null HEK cells transfected with the R/A mutant of YFP-labeled PAR2 (P1N-HEK/PAR2-Y-R/A) respond to 2-furoyl-LIGRLO-NH₂ (■, 1 μM) but do not respond to thrombin (▲, 25–50 U/ml) or to the PAR1-activating peptide TFLLR-NH₂ (○, 25 μM TF: added to cells predesensitized with 2fLI to eliminate the TF-mediated PAR2 calcium signal). **Tracing E:** Hirudin (◇, 2.5 μM) blocks the PAR2 response to thrombin (▲, 25 U/ml). **Tracing F:** Desensitizing P1N-HEK/PAR2Y-expressing cells by 2× treatment with 2-furoyl-LIGRLO-NH₂ (■, 5 μM) desensitizes the PAR2 response to thrombin (▲, 25 U/ml).

RIGHT PANELS G & H: G. Concentration-effect curves for thrombin activation of PAR2 calcium signaling in PAR1-null HEK cells expressing PAR2 (P1N-HEK/PAR2-Y) and HTB-9 cells (P1N-HTB-9). Increasing concentrations of thrombin were added to the PAR2-YFP-

MOL #102723

transfected PAR1-null cells (P1N-HEK/PAR2-Y: ●, Tracing to left) or the PAR1-null HTB-9 cells (P1N-HTB-9: right-hand curve), and the calcium signal was measured relative to the signal in the same cells triggered by 2 μ M ionophore (% A23187). Values represent the means of duplicate measurements in an assay wherein the spread of values was smaller than the symbols.

H. Relaxant response (Tension, g: downward deflection) due to thrombin activation of PAR2 (Thr ▲, 10 U/ml) in PAR1-null endothelium-intact mouse aorta rings constricted with phenylephrine (PE: 2.5 μ M: upward arrow). Desensitizing the PAR2 relaxant response by 2 \times exposure to the PAR2-activating peptide, 2fLIGRLO-NH₂ (2fLI: ■, 5 μ M), abrogated the response to thrombin. The scale for tension (g) and time (5 min) are shown by the inserted arrows.

Figure 4: Thrombin activation of PAR2 stimulates MAPKinase signaling in PAR2-expressing KNRK cells (KNRK-PAR2). Using previously described methods (Ramachandran et al., 2009; Mihara et al., 2013), KNRK cells, which do not respond to thrombin, were transfected with either PAR2 (left-hand western blot) or PAR2 (right-hand western blot), and the PAR-expressing cell lines so derived were treated with thrombin (2 or 20 U/ml). **A Western blots:** Cells were lysed after 10 min, and the activation of MAPKinase was measured by western blot analysis (P-MAPK) as described previously. **B Densitometry of bands:** P42/44 phospho-MAPKinase-ERK 1/2 bands were quantified densitometrically, and MAPKinase-ERK 1/2 activation was expressed as an increase relative to the signal observed in untreated samples. (Factor increase in p-ERK 1/2 over baseline). Histograms represent the average fold increase \pm s.e.m. (bars: $P \leq 0.05$ for all histogram values compared with untreated samples) for three replicate experiments.

MOL #102723

Figure 5: Thrombin-mediated PAR2-beta-arrestin interactions. PAR2, C-terminally tagged with eYFP (P2Y) was transfected into the PAR1-null HEK cells (P1N-HEK/P2Y) along with *Renilla reniformis* luciferase-tagged arrestin 1 or arrestin2. Bioluminescence resonance energy transfer between the receptor and either beta-arrestin 1 (Arr1) or beta-arrestin 2 (Arr2) (BRET Ratio nLuc/YFP) was then measured as described previously (Hamdan et al., 2005; Ramachandran et al., 2009) and in Materials and Methods. Histograms represent the average fold increase \pm s.e.m. (bars: $P \leq 0.05$ for all histogram values compared with thrombin-untreated samples) for three replicate measurements on independently grown cell samples.

Figure 6: Visualizing PAR2 activation by thrombin that cannot cleave the R36A PAR2 mutant: HEK cells expressing dual-tagged wild-type PAR2 (RFP-P2Y: Panels 1,2) or the cleavage-resistant dual-tagged PAR2 alanine mutant (RFP-P2Y-R/A: Panels 3,4)- were exposed (Panels 2,4) or not (Panels 1,3) to thrombin (Thr: 50 U/ml) for 30 min at room temperature. The intact receptor retaining the N-terminal mRFP tag along with the C-terminal eYFP tag appears yellow. When the mRFP tag is released by PAR2 cleavage/activation, the receptor appears green at the cell membrane and begins to cluster/internalize. Intact intracellular receptor in the golgi appears yellow. Representative imaging fields are shown for untreated (panels 1 and 3) and thrombin-treated (panels 2 and 4) monolayers. Trypsin (5U/ml) generated comparable image results for the wild-type and cleavage-resistant R/A PAR2 mutant (not shown). Bar in Panel 4: 2 μ m.

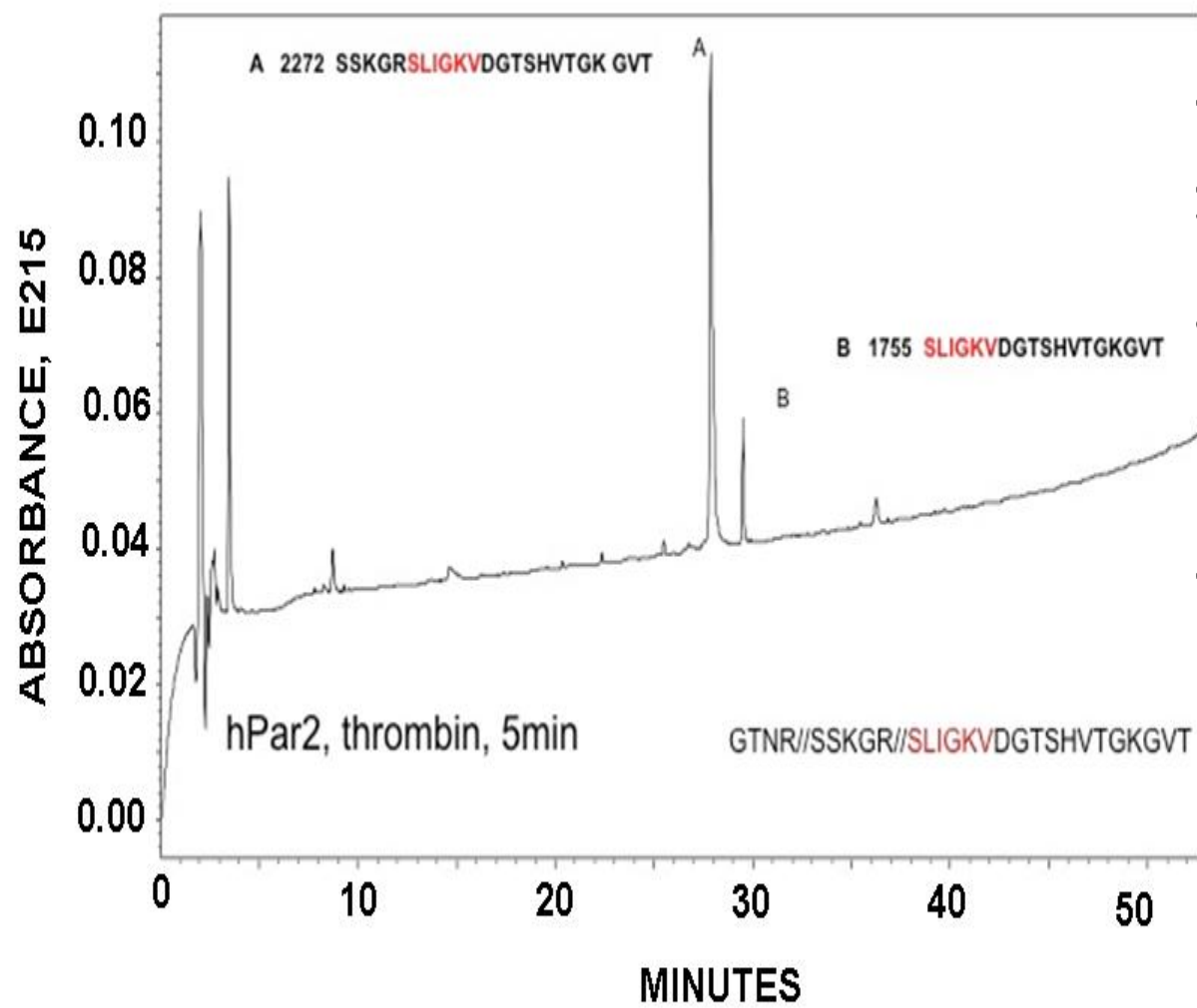


Figure 1

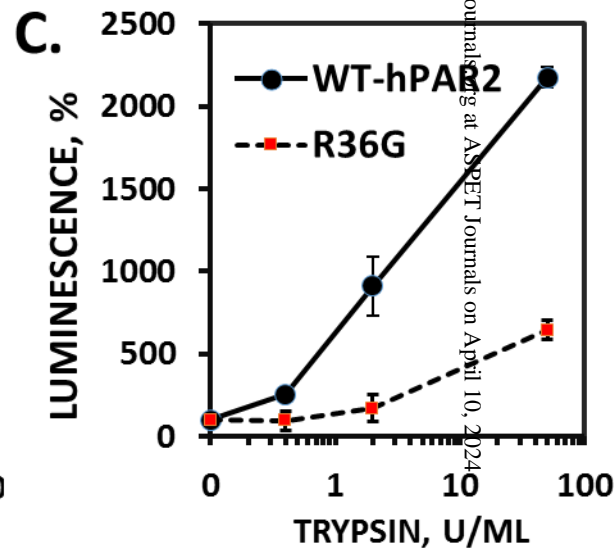
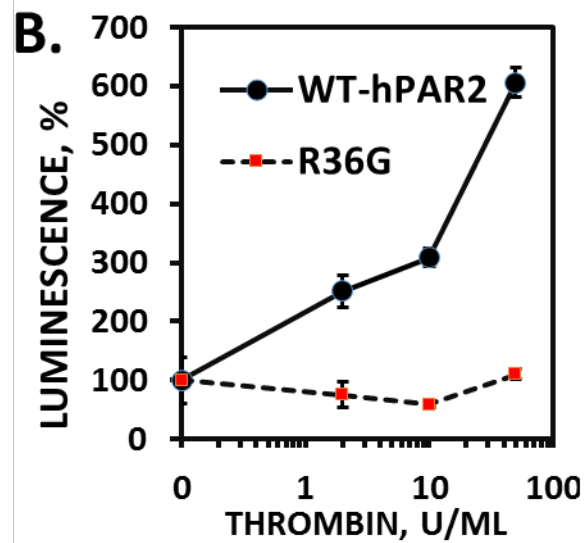
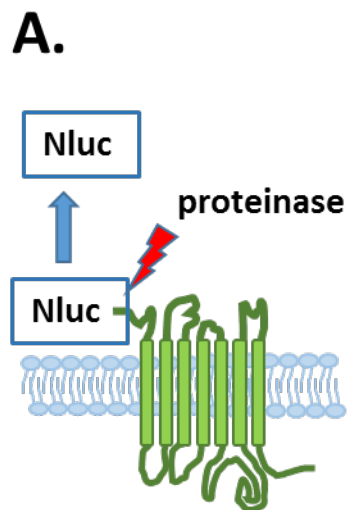


Figure 2

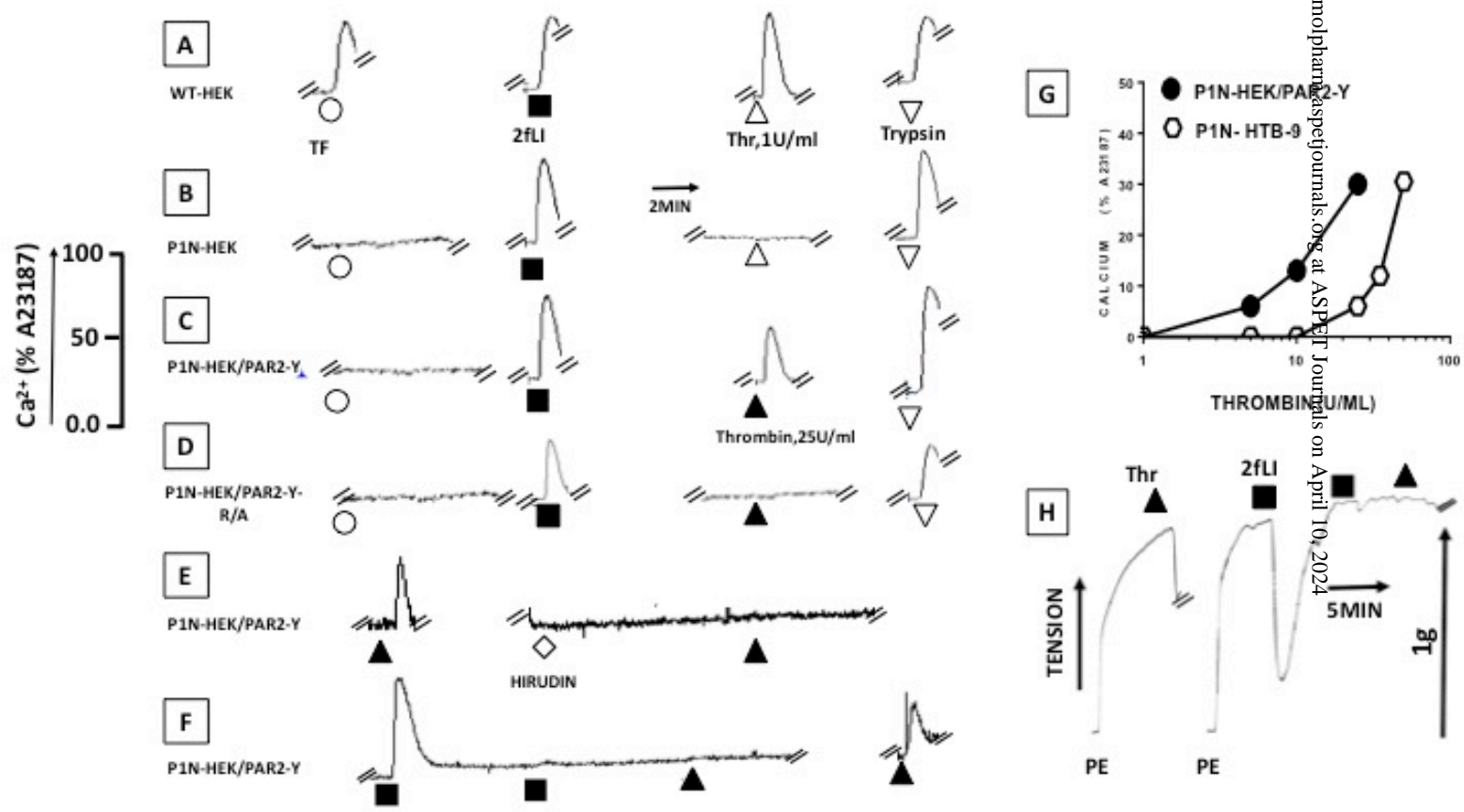


Figure 3

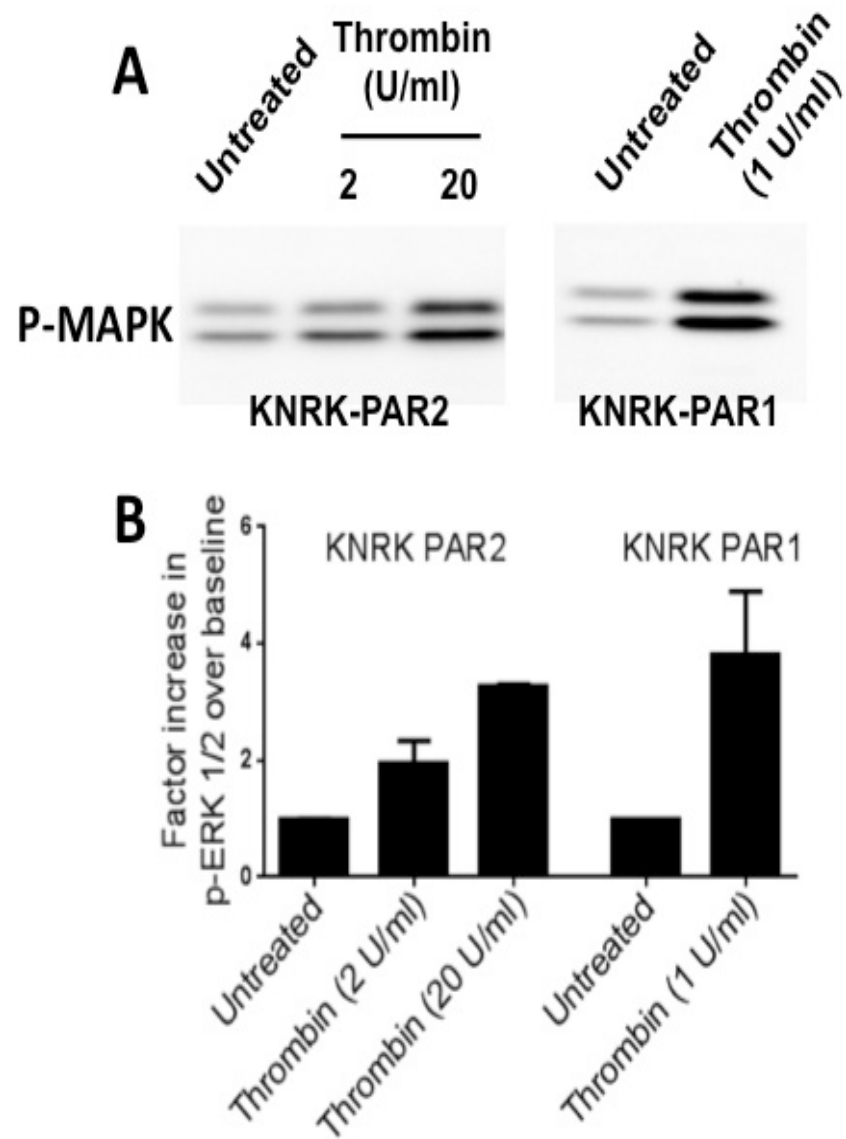


Figure 4

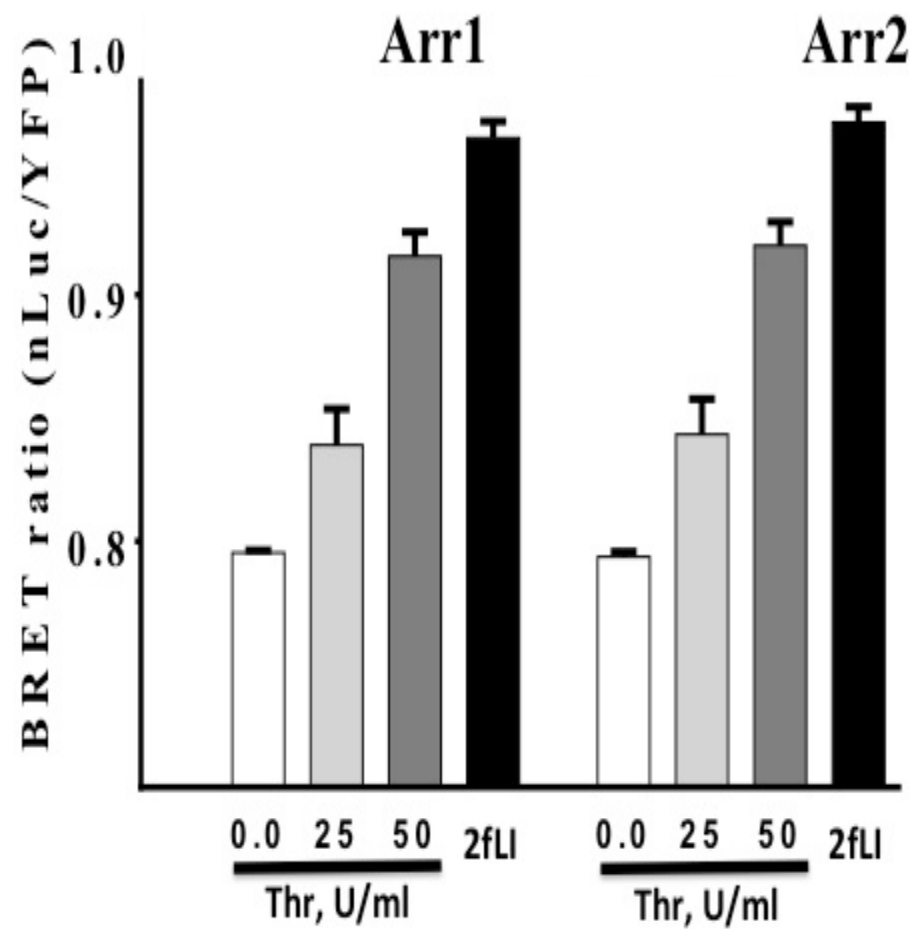


Figure 5

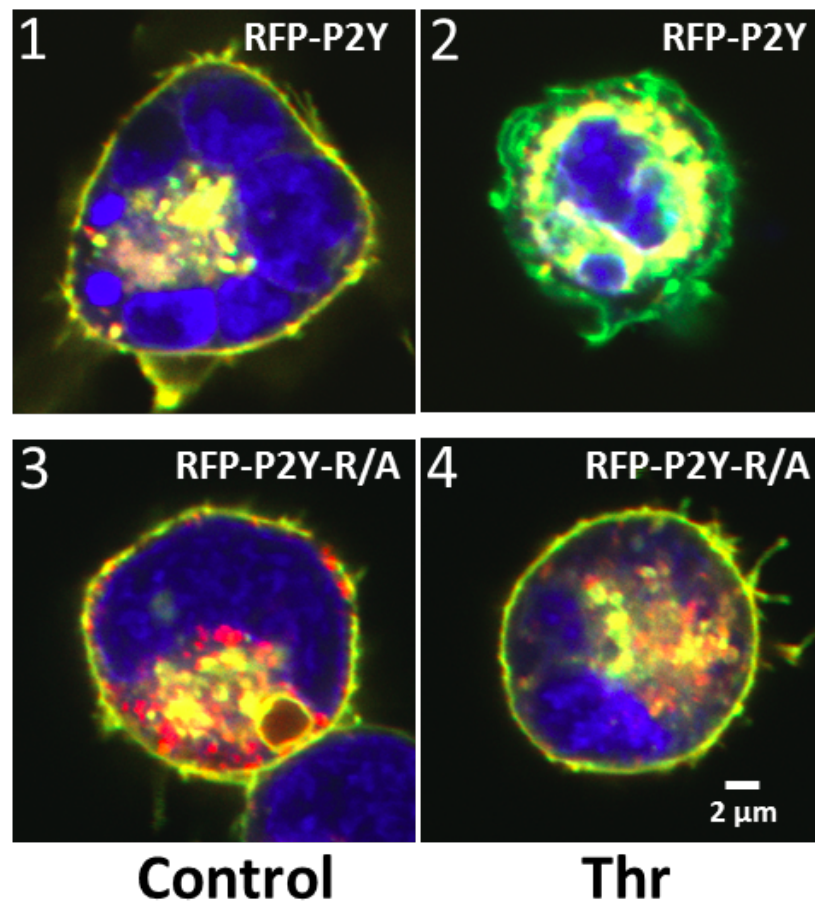


Figure 6